Title Page

Improved Analysis of Manganese in Steel Samples Using Collinear Long–Short Double Pulse Laser-Induced Breakdown Spectroscopy (LIBS)

Minchao Cui[1, 2], Yoshihiro Deguchi[2], Zhenzhen Wang[2, 3], Seiya Tanaka[2], Yuki Fujita[2], Shengdun Zhao[1]

[1]School of Mechanical Engineering, Xi'an Jiaotong University, Xi'an 710049, China

[2]Graduate School of Advanced Technology and Science, Tokushima University, Tokushima 770-8501, Japan

[3]State Key Laboratory of Multiphase Flow in Power Engineering, Xi'an Jiaotong University, Xi'an 710049, China

Corresponding author: Yoshihiro Deguchi

Graduate School of Advanced Technology and Science, Tokushima University

TEL: (+81)-88-656-7375

FAX: (+81)-88-656-9082

Email address:ydeguchi@tokushima-u.ac.jp

Postal address: 2-1, Minamijyosanjima, Tokushima 770-8506 Japan

Abstract

A long-short double pulse laser-induced breakdown spectroscopy (long-short DP-LIBS) method was employed to improve the performance of LIBS for the measurement of manganese in steel samples. The long pulse was generated by a Nd:YAG laser which was operated at free runing (FR) mode. To investigate the detection ability without sample preparation, the steel washers were tested using SP-LIBS and long-short DP-LIBS, respectively. The measurement results show that the long-short DP-LIBS method was able to record clear spectra from the rusty steel washers. The steel washers were also measured after the polishing process. The measurement results show that the signal intensity was enhanced by long-short DP-LIBS. Through the observation with scanning electron microscope (SEM) on the laser craters, the results suggest that the improvement of detection ability can be attributed to the pre-radiation effect of long-pulse laser beam. Next, the analytical performance for quantitative measurement of manganese was evaluated by employing ten standard steel samples. The results show that the linearty fit (R^2) of calibration curve is 0.988 for long-short DP-LIBS, whereas, R^2 is only 0.810 for SP-LIBS under the same measurement conditions. The five times repeated measurement results show that the average Relative Standard Deviation (RSD) of the tested samples is 29.3% for SP-LIBS and is 10.5% for long-short DP-LIBS. The prediction results also show that the average Relative Error of Prediction (REP) is 94.9% for SP-LIBS and it 4.9% for long-short DP-LIBS. The experimental results in current work demonstrate that long-short DP-LIBS is promising for the on line measurement of steel in the steelmaking plant.

Keywords: long-short DP-LIBS, steel, manganese, improvement, analytical performance, quantitative analysis

How many keywords? Please check the requirement of the journal.

1. Introduction

It is well known that the iron and steel industry is one of the most important industries. In modern life, steel products are used almost everywhere. With the development of industry, high quality steel is desired in various fields. The advanced control methods for steelmaking process are required to meet these industrial demands. However, it is difficult and expensive to measure the composition of steel during the steelmaking process, which limited the production efficiency of high quality steel. In recent years, laser-induced breakdown spectroscopy (LIBS), as one of the analytical techniques for steelmaking process, has been widely studied because of its potential for online analysis [1, 2]. Various papers have been published to report the applications of LIBS in steel industry, such as the measurements of solid steel [3-9], liquid steel [10-12], slags [13-15], oxides [16-18], rapid in-suit analysis [19-21], *etc.* One vital subject among these studies is the analytical performance of LIBS for the industrial application. To improve the performance, many approaches have been developed based on LIBS, such as microwave-assisted LIBS [22, 23], LIBS laser-induced fluorescence [24], resonance-enhanced LIBS [25, 26], double pulse LIBS [27-33], *etc*. However, it is still difficult to apply LIBS in the steelmaking process due to the terrible measurement conditions in steel plant. Double pulse LIBS (DP-LIBS) is a promising way to enhance the detection performance in practical application. Many geometrical configurations, such as reheating [27], collinear [28, 29], crossed beam [30], *etc*. have been studied to realize DP-LIBS. Among these configurations of DP-LIBS, the collinear configuration is feasible for the application in steel production lines [2]. However, the plasma conditions are still temporally unstable and spatially non-uniform [34, 35].

As well known, the theory of LIBS process is quite complex since several physical processes are involved in the generation and evolution of plasma, such as photon ionization, high velocity impact between electrons, atoms, molecules and ions, and inverse bremsstrahlung. The complete physical-mathematical model, which can finely describe the LIBS process, has not been established till now [36]. The unstable and non-uniform laser-induced plasma leads to the unsatisfied performance of LIBS for industrial requirements. Even though the temperature in plasma core is very high (10^4 K magnitude), the temperature in plasma edge is still very low (only a few thousand Kelvin) [37]. LIBS utilizes the signals which are emitted from the non-uniform plasma. However, at present, most of the quantitative analysis methods for LIBS assume that the laser-induced plasma is under the local thermodynamic equilibrium (LTE) condition. LTE condition means that the temperature of plasma can be considered as the same

value in a local region. In LIBS measurement, the laser-induced plasma sometimes does not meet LTE condition due to the pulsed laser beam. In previous reports, several works have obtained the high-accuracy results for quantitative analysis through considering unstable plasma conditions [37-39]. To solve the problem of unstable plasma in LIBS process, the collinear long-short DP-LIBS method was studied in previous work. A free oscillation long laser pulse combined with a Q-switched short laser pulse was employed to generate a stable plasma for spectral analysis. The feasibility of this method has been verified through the experiments in air and under water. The results have suggested that the plasma cooling process was controlled by the long-pulse-width laser [40, 41].

In order to remove the upper surface layer of measurement material, the approach to combine the long pulses with short pulses has been published since 2010 [42]. The two-phase measurement scheme with first cleaning long pulses and the second analysis laser pulses was applied to the analysis of as-cast layers on a steel bloom [8]. However, the long-short DP-LIBS method studied in present work employed the simultaneous combination of long and short pulses. A long laser pulse with the duration in microsecond time scale and a Q-switched short pulse with the duration in nanosecond time scale were both involved in the plasma generation and evolution processes. The long pulse laser beam continuously irradiates the plasma region before and after the plasma generation. To our knowledge, the analytical performance for the quantitative analysis has not been discussed in this configuration. The primary goal of current study is to evaluate the performance of collinear long-short DP-LIBS for the quantitative analysis of manganese in steel samples. Therefore, the comparative study has been carried out from several aspects between SP-LIBS and long-short DP-LIBS. The detection ability and the morphology of craters were studied by testing the steel washers with rusty and clean surface. Furthermore, this work reports a detailed discussion on the quantitative measurement of manganese in steel samples employing the standard steel samples.

2. Experimental setup for long-short DP-LIBS

2.1 Long-short DP-LIBS method

In this work, the long-short DP-LIBS method was employed to analyze the manganese content in steel samples. The long pulse in this method means that the duration time of laser pulse is long but the peak power is low. More specifically, the nanosecond Nd: YAG laser operated at free running (FR) mode was used as the long-pulse-width laser. The FR mode means that the Q value of optical resonant cavity does not change during

laser pulse formation. Thus the laser pulse can be sustained for dozens of microseconds with low peak power. This is also called as the free oscillation output of the laser. It is one of the working modes of Nd: YAG laser, but rarely used in LIBS process. Fig. 1 illustrates the principle of long-short DP-LIBS and the measured pulses shape of the long-short double pulses. The long pulse laser was irradiated before the short pulse irradiation and lasted for tens of microseconds after the short pulse irradiation ~~(plasma generation)~~. It is expected for long-short DP-LIBS to have two types of effect on LIBS process. One is the pre-radiation effect which includes the cleaning of loose surface layer and preheating the surface. The other ~~Another type~~ is the effect on the plasma evolution and cooling processes. The short pulse laser is irradiated at the middle of long pulse irradiation and generates the plasma from the cleaned and pre-heated surface. Moreover, once plasma is generated, the long-pulse width laser beam continuously irradiates the plasma region and provides the laser energy during the plasma evolution and cooling processes. Thus the plasma becomes stable for a certain time and the temperature can be maintained at a higher level [41]. With a suitable gate delay time, the signal from the plasma can be stably recorded by detector. In the literature of conventional DP-LIBS, it is reported that the plasma temperature has been enhanced [20], the plasma volume has been increased and the lasting time of the plasma emission has been extended [32, 43]. ~~It is proved that~~ The second Q-switched pulse mainly interacted with sample surface and the re-heating effect of the second Q-switched pulse was not observed [32]. However, the long pulse irradiation used in long-short DP-LIBS is a free-running laser pulse. Over tens of micro second range of time, it cleans and heats the surface ~~condition~~ of the sample before the plasma generation, the evolution and cooling processes of plasma after plasma generation [40, 41].

[insert Figure 1]

2.2 Experimental configuration

The experimental setup of the collinear long-short DP-LIBS configuration is shown in Fig.2. The measurement system was composed of two lasers, a digital delay generator, an optical fiber, a spectrometer, an ICCD (Intensified Charge Coupled Device) camera, a rotation sample stage and other auxiliary devices. The nanosecond Nd: YAG laser 1 (LOTIS TII, LS-2137U, 10 Hz, beam diameter: 8 mm) was operated at 1064 nm under the free-running (FR) mode. At this mode, the laser oscillation is freely output in a relatively long duration. Generally the energy density of free-running laser pulse is not sufficient to generate an observable plasma emission[40]. Thus the FR mode has been rarely used in LIBS ~~mode~~. In this work, the pulse energy of long pulse was set to 200

mJ with the pulse width of 60 μs. The nanosecond Nd: YAG laser 2 (LOTIS TII, LS-2134UTF, 10 Hz, beam diameter: 6 mm) was operated at 1064 nm (Q-Switch, pulse width 5.4 ns) with the pulse energy of 20.5 mJ. The inter-pulse delay time between the two lasers was adjusted by the digital delay generator (Stanford Research Systems, Model DG645). The pulse shape was measured and verified by an oscilloscope (Tektronix, MDO3014) with a Si photodiode sensor (Hamamatsu, S1336-18BQ). The long-pulse-width laser beam and the short-pulse-width laser beam were combined using a polarization prism and transmitted about 3 meters in air through the reflection of mirrors. The combined beams were focused on the samples with collinear configuration by a lens (focal length 800 mm). The emission signal from the plasma was collected in the reverse direction and focused on the fiber by using a lens (focal length 100 mm). After delivered 10 meters through the optical fiber, the emission signal was detected by the combination of a spectrometer (SOL, NP-250-2M), an ICCD camera (Andor, iStar DH334T-18U-03), and auxiliary devices. The delay time of ICCD was triggered by the short-pulse-width laser. A grating with 3600 grooves/mm was employed for spectral dispersion in the spectrometer. The system has achieved a spectral resolution of 0.0097 nm/pixel in the spectral range of 400-410 nm. All the spectra were recorded in open atmosphere.

[insert Figure 2]

2.3 Samples

In this work, two kinds of samples were measured to evaluate the performance of long-short DP-LIBS. The first kind of samples were steel washers which were made by industrial steel materials (Japan Grade: SS 330). Before experiments, the steel washers were placed in the environment of university factory for a long time, whereas, some of them had been polished using an abrasive paper. The purpose of measurement on steel washers was to qualitatively discuss the detection ability of long-short DP-LIBS in different surface conditions. The other kind of samples were standard steel samples by Zhengzhou Research Institution of Mechanical Engineering (ZRIME). The elementary composition of the samples is listed in Table 1. The iron concentration was calculated by other major element concentrations. There can be uncertainty in iron concentration due to some unreported minor elements. However, the uncertainty in iron concentration was neglected in the present study. Before the LIBS measurement, the standard steel samples were finely polished with the abrasive paper. During testing, the target sample was placed on the sample stage and kept rotating. Thus the laser pulses were always

irradiated on the fresh surface. After each experiment, the laser craters were confirmed without overlap.

[insert Table 1]

3. Results and discussion

3.1 Detection ability

The steel washer which was placed in the factory has a mixed surface layer including rust, oil, dust, et al. This surface layer is loose and easy to clean. In this work, the detection ability of SP-LIBS and long-short DP-LIBS was qualitatively compared by testing the steel washers with mixed surface and polished surface. Fig. 3 shows the recorded spectra from the steel washers with mixed surface. SP-LIBS was unable to record a clear spectrum for further analysis. On the contrary, long-short DP-LIBS recorded a clear spectrum. Several spectral lines of iron and manganese can be distinguished from the spectrum of long-short DP-LIBS. The comparison of the recorded spectra from steel washers with mixed surface indicated that long-short DP-LIBS has the potential to analyze the target with mixed surface layer. The results suggest that long-short DP-LIBS enhances the ability of LIBS applicability with no sample preparation. These application may include actual steel products with rusty and dirty surface, molten metals with oxide layers and steel sheets in production line with oil film on surface.

[insert Figure 3]

Fig. 4 shows the recorded spectra from the steel washers with polished surface. The signal intensity was enhanced by long-short DP-LIBS. For the spectral lines with higher excitation energies, such as iron atom lines at 400.971, 401.453, 402.187, 402.472, 405.504, 407.663, 409.597 and 409.818 nm, manganese atom lines at 401.810, 404.136, 404.876 and 407.924 nm, the enhancement was considerable. Enhancement in signal intensity of the spectral lines with lower excitation energies, such as iron atom lines at 400.524, 404.581, 406.359 and 407.174 nm, manganese atom lines at 403.076, 403.307 and 403.449 nm, was also observed although the enhancement was not as dramatic as for the spectral lines with higher excitation energies. The enhancement can be attributed to the effects of long pulse. For long-short DP-LIBS, the long pulse pre-heated the focus point on sample surface before the short pulse was irradiated, thus the breakdown threshold of material was reduced. Furthermore, the long pulse laser continues to irradiate the plasma region after the short pulse laser generates the plasma. The evolution and cooling processes of plasma were controlled by the long pulse hence the

plasma was maintained at higher temperature [41]. Because of the larger ablation mass and the higher plasma temperature, the signal intensity from the plasma was enhanced. Especially for the spectral lines with higher excitation energies, the enhancement was remarkable.

[insert Figure 4]

In addition, another result is worth to be noticed in Fig. 3 and Fig. 4. Long pulse LIBS, in which only the free-running laser pulse was irradiated to the target, was not able to record observable emission spectrum from the samples. It indicated that only the long pulse laser didn't generate the observable plasma because of the low irradiance. The result demonstrates that the plasma in the long-short DP-LIBS process was generated by the short pulse, although the long pulse was irradiated firstly. The plasma was generated by short pulse and affected by long pulse in long-short DP-LIBS process.

3.2 Crater morphology

The study on the crater morphology was carried out in this work. Scanning electron microscope (SEM) was employed to take the pictures of laser craters. Fig. 5 shows the observed images from the steel washers. A definite difference in crater characteristic from the steel washers with mixed surface was observed. A large area of surface layer was removed from the steel washers by long-short DP-LIBS. However, only short-pulse laser beam was unable to efficiently remove the surface layer. Therefore, the improvement of detection ability of long-short DP-LIBS can be attributed to the pre-radiation effect of long-pulse laser irradiation. Fig. 5(b) shows the crater images observed from the polished steel washers. A large area of laser ablation was observed in the image of long-short DP-LIBS craters. It is an evidence of the pre-radiation effect of long-pulse laser beam. The large ablation area of long-short DP-LIBS can be attributed to the efficient ablation under the pre-heating of long pulse, a large size of the focus spot of long pulse, the back expansion of the stronger plasma. The long-pulse laser beam affected the generation process of plasma from multiple aspects. These effects are collectively referred to the pre-radiation effect.

[insert Figure 5]

3.3 Calibration curves

The calibration curves for SP-LIBS and long-short DP-LIBS were compared in this study. All of the data obtained from 10 samples were used to establish the calibration curves. The experiment for each sample was repeated 5 times to reduce the influence of ~~unstable~~ laser energy conditions. The selected spectral lines (Mn I 404.876 nm and

Fe I 402.187 nm) were used to calculate the intensity ratio of LIBS measurement. Fig. 6 shows the calibration curves for SP-LIBS and long-short DP-LIBS. The ~~goodness of~~ linearity fit (R^2) of calibration curve was only 0.810 for SP-LIBS, whereas it was 0.988 for long-short DP-LIBS. From this aspect, the linearity of calibration curve was dramatically improved by long-short DP-LIBS. In Fig. 6(a), R^2 was lower than 0.9, which meant a weak correlation between the concentration ratio and the line intensity ratio. SP-LIBS did not obtain a satisfactory calibration curve for quantitative analysis due to the long optical distance in our experiments. A lens with the focus length of 800 mm was employed to focus the laser beam in this study. The emitted light of plasma was collected in the opposite direction of laser radiation. The long focus distance reduced the energy density of the focus point and resulted in a decrease in the stability of plasma signal. Therefore, the calibration curve obtained by SP-LIBS can't be used for further quantitative analysis. However, the long-short DP-LIBS method has obtained the acceptable calibration curve for quantitative analysis. The improvement in the quantitative analysis performance was attributed to the effects of long-pulse laser beam. These effects include not only the pre-radiation effect mentioned in Section 3.2 but also the stabilization effect. The long pulse irradiation continued for tens of microseconds in the long-short DP-LIBS method, thus it continuously provided long pulse laser energy to the plasma region throughout the life of the plasma. During this period, several mechanisms were involved to the plasma evolution process, including the absorption of laser energy by plasma and the heating of the sample surface by transmitted laser light. These mechanisms create a good environment for the plasma generation and evolution process and lead to a stabilized plasma condition.

Comparing the slope of the calibration curves, it can be found that the slope of long-short DP-LIBS was larger than that of SP-LIBS. This result suggests that the self-absorption influence was reduced by long-short DP-LIBS. In LIBS, the local temperature in a plasma varied with the spatial location. Generally, the temperature in the outer region of plasma is lower than the core region. The emission from the core plasma could be absorbed by the outer plasma. Therefore, it is reported that LIBS has suffered the influence of self-absorption, which caused a decrease in the slope of calibration curve [37, 44, 45]. Obviously, the measurement results were less affected by self-absorption using long-short DP-LIBS. It can be attributed to the stabilization effect of long pulse. In long-short DP-LIBS, the plasma is continuously irradiated by the long-pulse-width laser, hence the evolution and cooling processes of plasma are controlled [41]. The stability of plasma is improved by the long pulse. Therefore, the self-absorption influence was weakened in long-short DP-LIBS. In addition, it can be

found in Fig. 6 that the standard deviations of measurement result are smaller in long-short DP-LIBS, which also can be attributed to the stabilization effect of long pulse.

[insert Fig. 6]

3.4 Precision and uncertainty of measurement

The prediction models for manganese concentration were evaluated using the cross validation method. The unknown sample was selected from S2 sample to S9 sample individually, and the remaining 9 samples were employed to establish the prediction model. Fig. 7 shows the prediction models for manganese concentration using SP-LIBS. The linearity fit (R^2) of the prediction models were all lower than 0.9, except for that of the prediction model for S7 sample. The quantitative analysis based on these prediction models are unreliable under such low R^2 value. Fig. 8 shows the prediction models using long-short DP-LIBS. It can be seen that all of the models have obtained a fine R^2 value. These results suggest that the analytical performance of manganese in steel samples by long-short DP-LIBS.

[insert Fig. 7]

[insert Fig. 8]

To quantitatively compare the precision and uncertainty of measurement between SP-LIBS and long-short DP-LIBS, the statistical factors like Relative Standard Deviation (RSD) and Relative Error of Prediction (REP) were calculated in current study. More specifically, RSD was used to evaluate the precision of measurement and REP was used to evaluate the uncertainty of measurement. Precision is defined as the degree of harmonization among single test data when the measurement is carried out repeatedly [46]. Therefore, RSD was calculated according to the Eq. (1).

$$s = \left[\frac{\sum (x_i - M)^2}{n - 1} \right]^{1/2}$$

$$\text{RSD} = 100\% \times [s/M] \tag{1}$$

In these equations, x_i is the measured value from LIBS experiments, n is the number of parallel experiments, M is the average value of all parallel experiments, s is the standard deviation and RSD is the relative standard deviation.

Uncertainty describes the nearness of agreement between the measured experimental values and the reference value (either as a true value or the value observed by standard process). In this study, manganese concentration provided by ZRIME was used to

testify the uncertainty of measurement. REP was calculated using the following equation [47]:

$$\%\mathrm{REP} = \frac{100\%}{Y_\mathrm{m}} \sqrt{\frac{1}{N}\Sigma_{i=0}^{N}(Y_\mathrm{s} - Y_\mathrm{p})^2}$$ (2)

where Y_m is the average reference concentration of the prediction samples, N is total number of samples, Y_s is the reference concentration of the ith sample, Y_p is the prediction concentration using the established calibration model of the ith sample and REP is the relative error of prediction also known as relative average root mean square error. For a fine calibration model, REP should be as small as possible. The overall efficiency of calibration models was compared using REP in this study.

Table 2 shows a comparison of RSD and REP for SP-LIBS and long-short DP-LIBS. The precision and uncertainty of long-short DP-LIBS measurement were found to be better than those of SP-LIBS measurement. The average value of RSD was reduced from 29.3% to 10.5%, meanwhile, the average value of REP was reduced from 94.9% to 4.9%. In the literature of manganese quantitative analysis, it was reported that the relative error of manganese prediction was 7.2% using conventional DP-LIBS and univariate model [20], the relative standard error of manganese prediction was 10.32% using SP-LIBS and partial least squares regression model [48]. This result demonstrates that the use of long pulse is helpful for better analytical results of manganese. The improvement of measurement precision and uncertainty is attributed to the stabilized plasma using long-short DP-LIBS.

[insert Table 2]

4. Conclusions

The performance of collinear long-short DP-LIBS for the analysis of manganese in steel samples was studied in this work. According to the experimental results, the performance improvement was discussed in several aspects hence the conclusions are drawn as follows.

1. The long-short DP-LIBS has recorded the clear spectra from the steel washers which had the mixed surface layer with rust. Through the study on the crater morphology, the improvement of detection ability is attributed to the pre-radiation effect of long pulse laser.

2. The calibration curve of long-short DP-LIBS shows a larger slope. The linearty fit (R^2) is 0.988 for the calibration curve of long-short DP-LIBS, which is acceptable for

the manganese analysis. The larger slope of calibration curve for long-short DP-LIBS indicates that the influence of self-absorption was weakened by the long pulse, which improved the analytical performance of manganese.

3. The quantitative analysis of manganese shows that the precision and uncertainty of measurement was improved by long-short DP-LIBS. Mean RSD reduced from 29.3% to 10.5% and mean REP reduced from 94.9% to 4.9%.The improvement is attributed to the stabilized plasma which was generated by long-short DP-LIBS process. The simulated prediction results demonstrated that the analytical performance of manganese was improved by long-short DP-LIBS compared to the traditional SP-LIBS.

References

[1] R. Noll. Laser-Induced Breakdown Spectroscopy: Fundamentals and Applications. Springer-Verlag, Berlin Heidelberg, 2012.

[2] Y. Deguchi. Industrial Applications of Laser Diagnostics, CRS Press, Taylor & Francis: New York, 2011.

[3] J. Vrenegor, R. Noll, V. Sturm. "Investigation of matrix effects in laser-induced breakdown spectroscopy plasmas of high-alloy steel for matrix and minor elements". Spectrochim. Acta Part B 2005. 60: 1083-1091.

[4] C.M. Li, Z.M. Zou, X.Y. Yang, Z.Q. Hao, L.B. Guo, X.Y. Li, Y.F. Lu, X.Y. Zeng. "Quantitative analysis of phosphorus in steel using laser-induced breakdown spectroscopy in air atmosphere". J. Anal. At. Spectrom. 2014. 29: 1432-1437.

[5] H. Balzer, M. Hoehne, R. Noll, V. Sturm. "New approach to online monitoring of the Al depth profile of the hot-dip galvanised sheet steel using LIBS". Anal. Bioanal. Chem. 2006. 385: 225-233.

[6] M. A. Khater. "Laser-induced breakdown spectroscopy for light elements detection in steel: State of the art". Spectrochim. Acta Part B 2013. 81: 1-10.

[7] H. Balzer, S. Hölters, V. Sturm, R. Noll. "Systematic line selection for online coating thickness measurements of galvanised sheet steel using LIBS". Anal. Bioanal. Chem. 2006. 385: 234-239.

[8] C. Meinhardt, V. Sturm, R. Fleige, C. Fricke-Begemann, R. Noll. "Laser-induced breakdown spectroscopy of scaled steel samples taken from continuous casting blooms". Spectrochim. Acta Part B 2016. 123: 171-178.

[9] S. Yao, J. Lu, K. Chen, S. Pan, J. Li, M. Dong. "Study of laser-induced breakdown spectroscopy to discriminate pearlitic/ferritic from martensitic phases". Appl. Surf. Sci. 2011. 257: 3103-3110.

[10] J. Gruber, J. Heitz, H. Strasser, D. Bauerle, N. Ramaseder. "Rapid in-situ analysis of liquid steel by laser-induced breakdown spectroscopy". Spectrochim. Acta Part B 2001. 56: 685-693.

[11] L. Peter, V. Sturm, R. Noll. "Liquid steel analysis with laser-induced breakdown spectrometry in the vacuum ultraviolet". Appl. Optics. 2003. 42: 6199-6204.

[12] C. Aragon, J.A. Aguilera, J. Campos. "Determination of carbon content in molten steel using laser-induced breakdown spectroscopy". Appl. Spectrosc. 1993. 47: 606-608.

[13] P.J. Kolmhofer, S. Eschlböck-Fuchs, N. Huber, R. Rössler, J. Heitz, J.D. Pedarnig. "Calibration-free analysis of steel slag by laser-induced breakdown spectroscopy with combined UV and VIS spectra". Spectrochim. Acta Part B 2015. 106: 67-74.

[14] H. K. Sanghapi, K. K. Ayyalasomayajul, F. Y. Yueh, J. P. Singh, D. L. McIntyre, J. C. Jain, J. Nakano. "Analysis of slags using laser-induced breakdown spectroscopy". Spectrochim. Acta Part B 2016. 115: 40-45.

[15] C.M. Ahamer, S. Eschlböck-Fuchs, P.J. Kolmhofer, R. Rössler, N. Huber, J.D. Pedarnig. "Laser-induced breakdown spectroscopy of major and minor oxides in steel slags: Influence of detection geometry and signal normalization". Spectrochim. Acta Part B 2016. 122: 157-164.

[16] F. Boué-Bigne. "Laser-induced breakdown spectroscopy and multivariate statistics for the rapid identification of oxide inclusions in steel products". Spectrochim. Acta Part B 2016. 119: 25-35.

[17] A. Demidov, S. Eschlböck-Fuchs, A.Y. Kazakov, I.B. Gornushkin, P.J. Kolmhofer, J.D. Pedarnig, N. Huber, J. Heitz, T. Schmid, R. Rossler, U. Panne. "Monte Carlo standardless approach for laser induced breakdown spectroscopy based on massive parallel graphic processing unit computing". Spectrochim. Acta Part B 2016. 125: 97-102.

[18] J.D. Pedarnig, M.J. Haslinger, M.A.Bodea, N.Huber, H. Wolfmeir, J. Heitz. "Sensitive detection of chlorine in iron oxide by single pulse and dual pulse laser-induced breakdown spectroscopy". Spectrochim. Acta Part B 2014. 101: 183-190.

[19] N. Hubera, S. Eschlböck-Fuchsa, H. Scherndlb, A. Freimundb, J. Heitza, J.D. Pedarnig. "In-line measurements of chlorine containing polymers in an industrial waste sorting plant by laser-induced breakdown spectroscopy". Appl. Surf. Sci. 2014. 302: 280-285.

[20] L. Sun, H. Yu, Z. Cong, Y. Xin, Y. Li, L. Qi. "In situ analysis of steel melt by double-pulse laser-induced breakdown spectroscopy with a Cassegrain telescope". Spectrochim. Acta Part B 2015. 112: 40-48.

[21] F. Boué-Bigne. "Laser-induced breakdown spectroscopy applications in the steel industry: Rapid analysis of segregation and decarburization". Spectrochim. Acta Part B 2008. 63: 1122-1129.

[22] K. Ali, M. Tampo, K.Akaoka, M. Miyabe, I. Wakaida. "Enhancement of LIBS emission using antenna-coupled microwave". Opt. Express. 2013. 21: 29755-29768.

[23] Jan Viljanen, ZhiweiSun, Zeyad T. Alwahabi. "Microwave assisted laser-induced breakdown spectroscopy at ambient conditions". Spectrochim. Acta Part B 2016. 118: 29-36.

[24] H. Loudyi, K. Rifaï, S. Laville, F. Vidal, M. Chaker, M. Sabsabi. "Improving laser-induced breakdown spectroscopy (LIBS) performance for iron and lead determination in aqueous solutions with laser-induced fluorescence (LIF)". J. Anal. At. Spectrom. 2009. 24: 1421-1428.

[25] W. L. Yip, N. H. Cheung. "Analysis of aluminum alloys by resonance-enhanced laser-induced breakdown spectroscopy: How the beam profile of the ablation laser and the energy of the dye laser affect analytical performance". Spectrochim. Acta Part B 2009. 64: 315-322.

[26] C. Goueguel, S. Laville, F. Vidal, M. Sabsabi, M. Chaker. "Investigation of resonance-enhanced laser-induced breakdown spectroscopy for analysis of aluminium alloys". J. Anal. At. Spectrom. 2010. 25: 635-644.

[27] J. Uebbing, J. Brust, W. Sdorra, F. Leis, K. Niemax. "Reheating of a laser-produced plasma by a second pulse laser". Appl. Spectrosc. 1991. 45: 1419-1423.

[28] R. Sattmann, V. Sturm, R. Noll. "Laser-induced breakdown spectroscopy of steel samples using multiple Q-switch Nd:YAG laser pulses". J. Phys. D: Appl. Phys. 1995. 28: 2181-2187.

[29] G. Cristoforetti, S. Legnaioli, V. Palleschi, A. Salvetti, E. Tognoni. "Characterization of a collinear double pulse laser-induced plasma at several ambient

gas pressures by spectrally- and time-resolved imaging". Appl. Phys. 2005. 80: 559-568.

[30] Y. Lu, V. Zorba, X. L. Mao, R. Zheng, R. E. Russo. "UV fs–ns double-pulse laser induced breakdown spectroscopy for high spatial resolution chemical analysis". J. Anal. At. Spectrom. 2013. 28: 743-748.

[31] R. Sanginés, V. Contreras, H. Sobral, A. Robledo-Martinez. "Optimal emission enhancement in orthogonal double-pulse laser-induced breakdown spectroscopy". Spectrochim. Acta Part B 110(2015)139-145.

[32] R. Noll, R. Sattmann, V. Sturm, S. Winkelmann. "Space- and time-resolved dynamics of plasmas generated by laser double pulses interacting with metallic samples". J. Anal. At. Spectrom. 2004. 19: 419-428.

[33] V.N. Lednev, S.M. Pershin, A.F. Bunkin, A.A. Samokhvalov, V.P. Veiko, S.I. Kudryashov, A.A. Ionin. "Double pulse laser induced breakdown spectroscopy with Gaussian and multimode beams". Spectrochim. Acta Part B 2016. 124: 47-55.

[34] Chao Song, Xun Gao, Yan Shao. "Pre-ablation laser parameter effects on the spectral enhancement of 1064 nm/1064 nm dual-pulse laser induced breakdown spectroscopy". Optik 2016. 127: 3979-3983.

[35] X. Jiang, P. Hayden, R. Laasch, J.T. Costello, E.T. Kennedy. "Inter-pulse delay optimization in dual-pulse laser induced breakdown vacuum ultraviolet spectroscopy of a steel sample in ambient gases at low pressure". Spectrochim. Acta Part B 2013. 86: 66-74.

[36] T. Fujimoto. Plasma Spectroscopy, Oxford University Press on Demand, 2004.

[37] X.B. Zhang, Y. Deguchi, J.P. Liu. "Numerical simulation of laser induced weakly ionized helium plasma process by lattice boltzmann method". Jpn. J. Appl. Phys. 2012. 51: 01AA04-1-01AA04-6.

[38] O. Barthelemy, J. Margot, S. Laville, F. Vidal, M. Chaker, B. Le Drogoff, T.W. Johnston, M. Sabsabi. "Investigation of the State of Local Thermodynamic Equilibrium of a Laser-Produced Aluminum Plasma". Appl. Spectrosc. 2005. 59: 529-536.

[39] M. Skočić, S. Bukvić. "Laser Induced Plasma Expansion and Existence of Local Thermodynamic Equilibrium". Spectrochim. Acta Part B 2016. 125: 103-110.

[40] Z. Wang, Y. Deguchi, R. Liu, A. Ikutomo, Z. Zhang, D. Chong, J. Yan1., J. Liu, F.J. Shiou. "Emission characteristics from laser-induced plasma using collinear long and short dual-pulse LIBS". Appl. Spectrosc. 2017. 71(9): 2187-2198.

[41] M. Cui, Y. Deguchi, Z. Wang, Y. Fujita, R. Liu, F.J. Shiou, S. Zhao. "Enhancement and stabilization of plasma using collinear long-short double-pulse laser-induced breakdown spectroscopy". Spectrochim. Acta Part B 2018. 142: 14-22.

[42] Ü. Aydin, R. Noll, J. Makowe, R. Kelnberger. Method for preparing laser material removal, particularly for executing laser-emission spectroscopy, involves irradiating upper surface of object with one or multiple laser pulses, in order to remove upper surface section. German Patent No. DE102008032532.

[43] R. Noll, V. Sturm, Ü. Aydin, D. Eilers, C. Gehlen, M. Höhne, A. Lamott, J. Makowe, J. Vrenegor. "Laser-induced breakdown spectroscopy—From research to industry, new frontiers for process control". Spectrochim. Acta Part B 2008. 63: 1159-1166.

[44] Z. Hao, L. Guo, C. Li, M. Shen, X. Zou, X. Li, Y. Lu, X. Zeng. "Sensitivity improvement in the detection of V and Mn elements in steel using laser-induced breakdown spectroscopy with ring-magnet confinemen". J. Anal. At. Spectrom. 2014. 29: 2039-2314.

[45] S.M. Zaytsev, A.M. Popov, E.V. Chernykh, R.D. Voronina, N.B. Zorov, T.A. Labutin. "Comparison of single- and multivariate calibration for determination of Si, Mn, Cr and Ni in high-alloyed stainless steels by laser-induced breakdown spectrometry". J. Anal. At. Spectrom. 2014. 29: 1417-1424.

[46] J.N. Miller, J.C. Miller. Statistics and Chemometrics for Analytical Chemistry, 6th ed., Prentice Hall, England, 2006.

[47] A. Sarkar, X.L. Mao, G. C.-Y. Chan, R. E. Russo. "Laser ablation molecular isotopic spectrometry of water for $_1D^2/_1H^1$ ratio analysis". Spectrochim. Acta Part B. 2013. 88: 46-53.

[48] A. S. Luna, F. B. Gonzaga, W. F.C. Rocha, I. C.A. Lima. "A comparison of different strategies in multivariate regression models for the direct determination of Mn, Cr, and Ni in steel samples using laser-induced breakdown spectroscopy". Spectrochim. Acta Part B. 2018. 139: 20-26.

Table 1 Elements composition of the standard steel samples

Sample	Content (%)				
No.	Mn	C	Si	Cr	Fe*
S1	0.032	0.0032	0.0031	0.0053	99.742
S2	0.440	0.085	0.217	0.104	98.755
S3	0.472	0.233	0.354	0.216	98.479
S4	0.752	0.454	0.444	0.141	97.720
S5	0.778	0.586	0.471	0.131	97.575
S6	0.842	0.276	0.560	0.362	96.996
S7	0.957	0.340	0.779	0.408	96.348
S8	1.12	0.192	0.363	0.201	97.519
S9	1.23	0.297	0.470	0.203	97.423
S10	1.36	0.332	0.716	0.154	97.007

Symbol '*' means the value was calculated by knowing the other major elements.

Table 2 Precision and uncertainty of measurement

Tested sample	RSD (%)		REP (%)	
	SP-LIBS	Long short DP-LIBS	SP-LIBS	Long short DP-LIBS
S2	30.1	18.6	75.7	1.1
S3	19.2	11.9	101.5	9.4
S4	38.3	6.0	83.9	3.8
S5	23.6	14.1	90.4	9.8
S6	31.0	5.0	95.4	2.8
S7	26.4	10.1	45.8	4.6
S8	24.9	11.8	169.0	2.2
S9	41.0	6.5	97.7	5.7
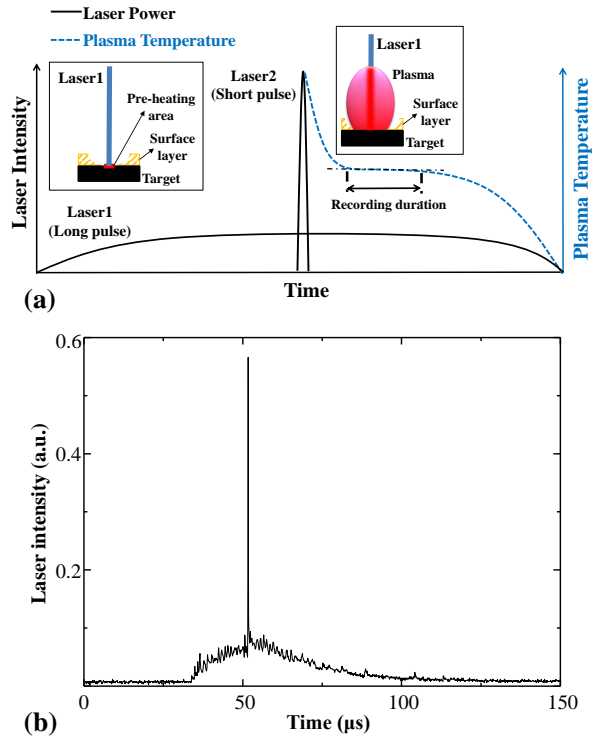
Fig. 1 Long-short LIBS method. (a) Schematic diagram and (b) measured long-short pulse shape.
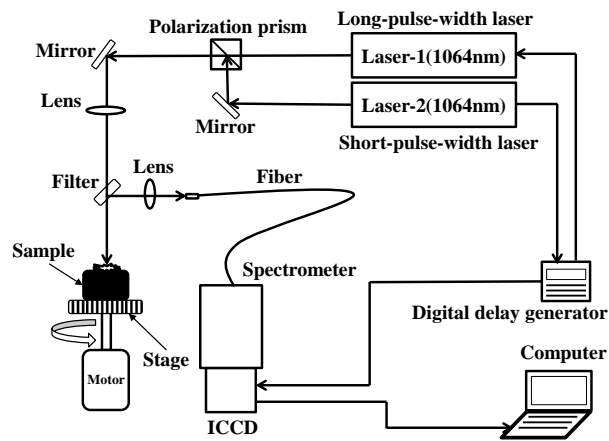
Fig. 2 Experimental setup for collinear long-short DP-LIBS configuration.
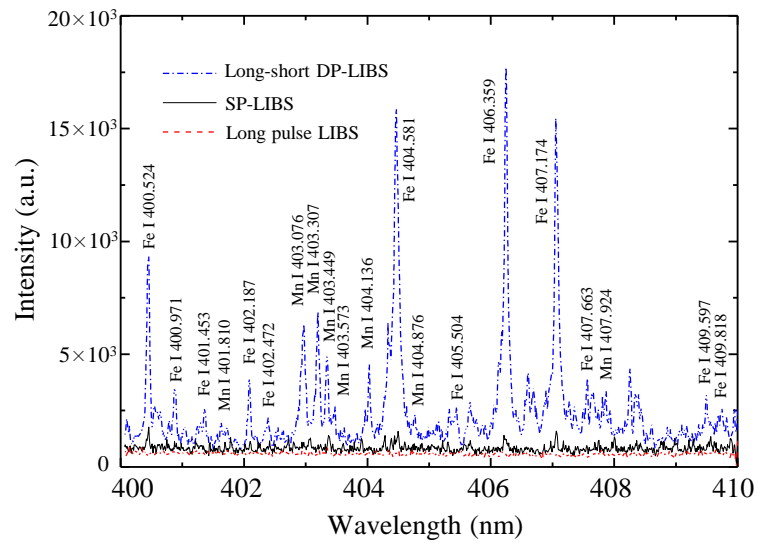
Fig. 3 Measured spectra from the steel washers with mixed surface. Experimental conditions: gate width: 1000 ns, accumulation: 20 times, delay time: 2000 ns, SP-LIBS pulse energy: 20.5 mJ; long-short DP-LIBS pulse energy: short pulse 20.5 mJ, long pulse 200 mJ; long pulse LIBS pulse energy: 200 mJ.
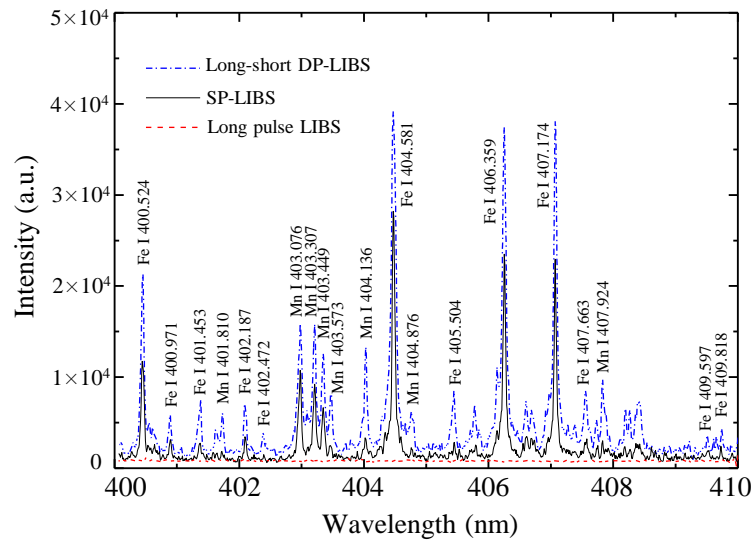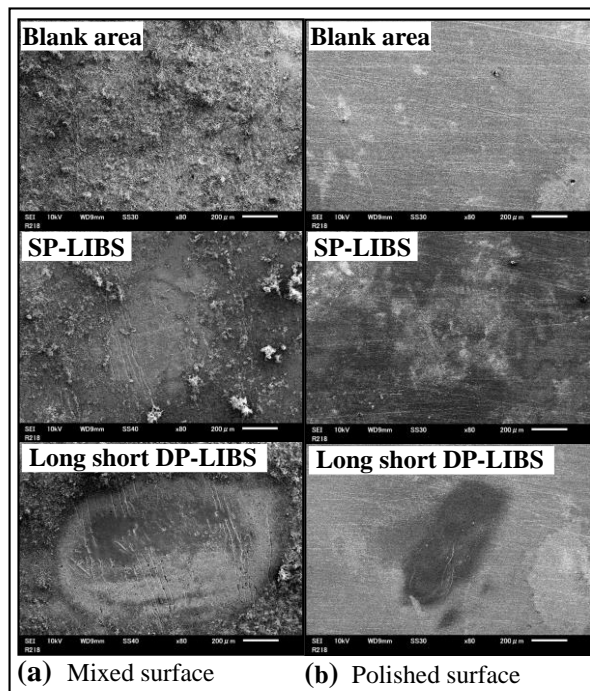
Fig. 4 Measured spectra from the steel washers with polished surface. Experimental conditions: gate width: 1000 ns, accumulation: 20 times, delay time: 2000 ns, SP-LIBS pulse energy: 20.5 mJ; long-short DP-LIBS pulse energy: short pulse 20.5 mJ, long pulse 200 mJ; long pulse LIBS pulse energy: 200 mJ.

Fig. 5 SEM images for laser craters. (a) Results from the steel washers with mixed surface and (b) results from the steel washers with polished surface.
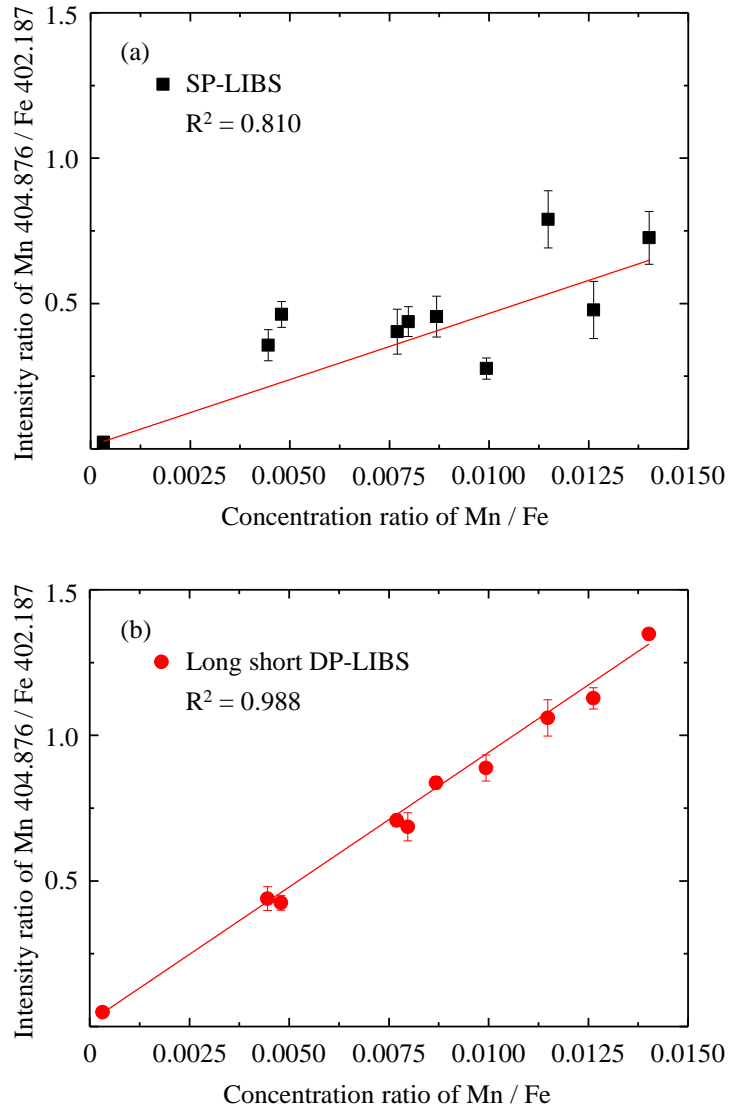
Fig. 6 Calibration curves for (a) SP-LIBS and (b) long-short DP-LIBS. Experimental conditions: gate width: 1000 ns, accumulation: 50 times, delay time: 4000 ns, SP-LIBS pulse energy: 20.5 mJ, long-short DP-LIBS pulse energy: short pulse 20.5 mJ, long pulse 200 mJ.
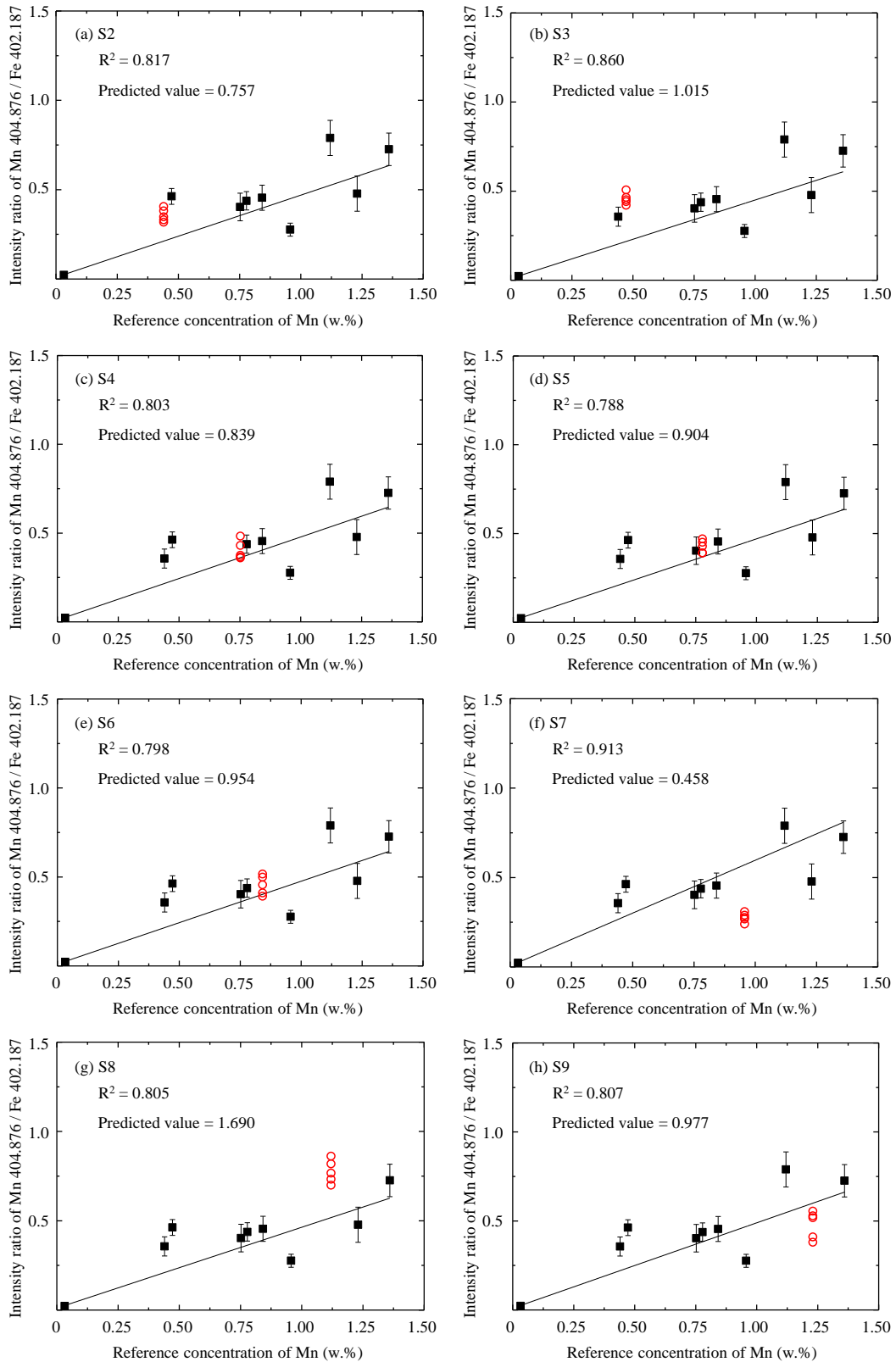
Fig. 7 Prediction models for SP-LIBS. (a-h) are the models for predicted sample (S2-S9), respectively. Experimental conditions: gate width: 1000 ns, accumulation: 50 times, delay time: 4000 ns, SP-LIBS pulse energy: 20.5 mJ, long-short DP-LIBS pulse energy: short pulse 20.5 mJ, long pulse 200 mJ.
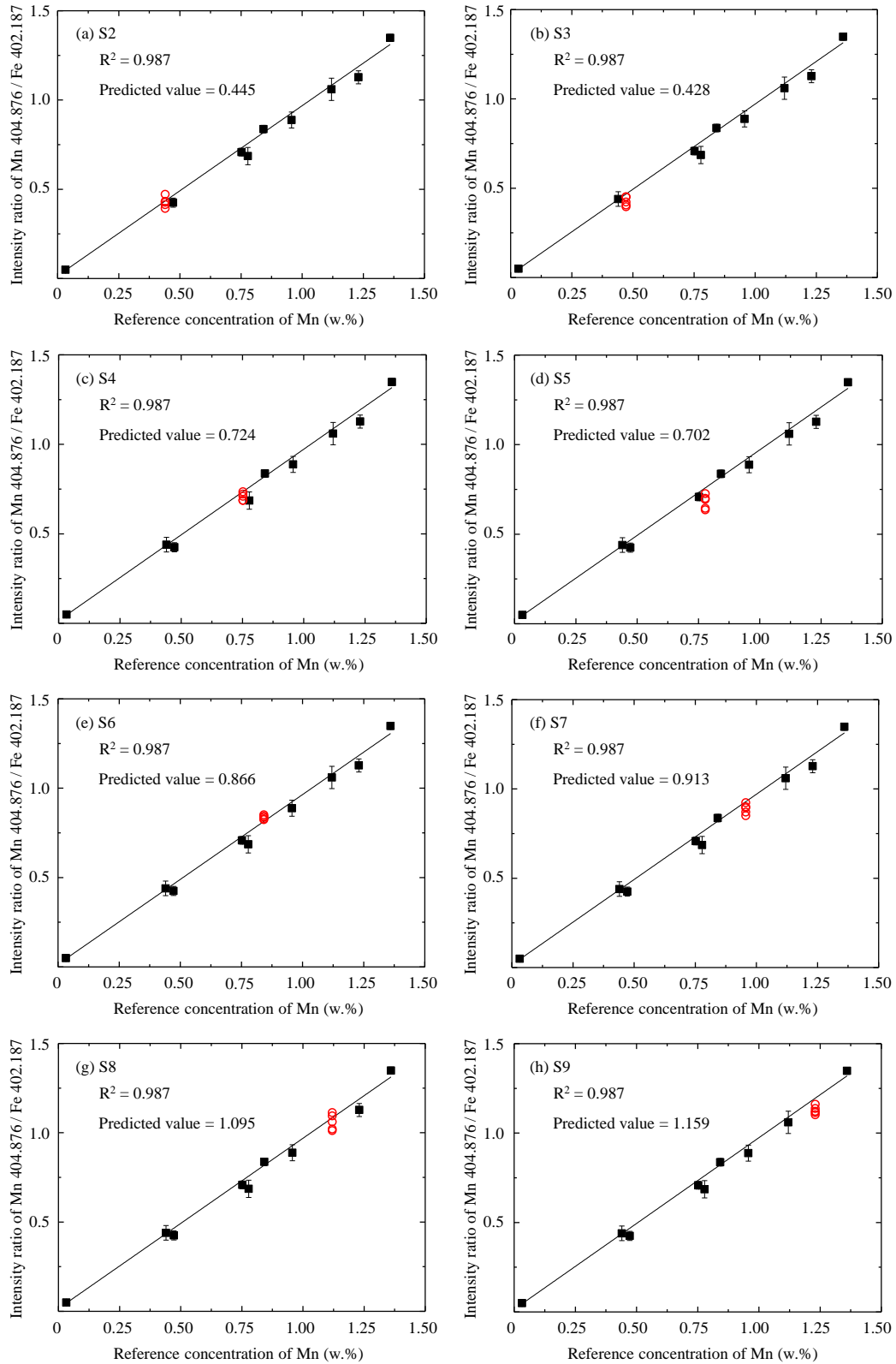
Fig. 8 Prediction models for long-short DP-LIBS. (a-h) are the models for predicted sample (S2-S9), respectively. Experimental conditions: gate width: 1000 ns, accumulation: 50 times, delay time: 4000 ns, SP-LIBS pulse energy: 20.5 mJ, long-short DP-LIBS pulse energy: short pulse 20.5 mJ, long pulse 200 mJ.